Chapter 10
Basic Magnetic and Mechanical Properties of Microwire Composites

## 10.1 Magnetic Properties of Composites

Due to the inclusion of magnetic fillers, the polymer composite becomes magnetic, i.e. responsive to the external static or dynamic magnetic field. Although most studies are devoted to the dynamic response of these kinds of heterogeneous composite media [1], i.e. complex permeability, it is worth exploring the static magnetic properties of microwire composites for two reasons: (i) the composite with wire arrays could be of some application interest in the magnetic sensing field, as quite a few studies are devoted to the microwire arrays [2–7]. (ii) ac permeability is associated with the static magnetic properties such as saturation magnetisation and the anisotropy field, according to the modified model based on Snoek's law proposed by Acher et al. [8, 9].

$$\int_{0}^{F} \mu''(f)f\mathrm{d}f \leq \frac{\pi}{6}\tau(\bar{\gamma}4\pi M_{\mathrm{s}})^2, \tag{10.1}$$

where μ is the imaginary part of complex permeability, f is the frequency, τ denotes the volume fraction of magnetic fillers, $\bar{\gamma}$ is the gyromagnetic factor with a value of 2.8 MHz/Oe, and M_{s} is the saturation magnetisation. In this connection, this section addresses some of the static magnetic properties of microwire composites.

Phan et al. [10] prepared E-glass prepreg-based composites with bundles of microwires and measured their magnetic properties in comparison with those of the single wires. Figure 10.1 shows the M–H curves of the single microwire and composite. It is interesting to note that, for both longitudinal and transverse measurements, the coercivity of the as-prepared composite is much smaller than that of the single microwire. This indicates better soft magnetic properties for the microwire composite than single wires. It is also shown that the effective anisotropy field for the bundles of microwire is strongly increased as compared to the single wire

Fig. 10.1 Comparison of magnetic hysteresis loops of a single magnetic microwire and its as-prepared composite. Reproduced with permission from [10], copyright 2007 AIAA
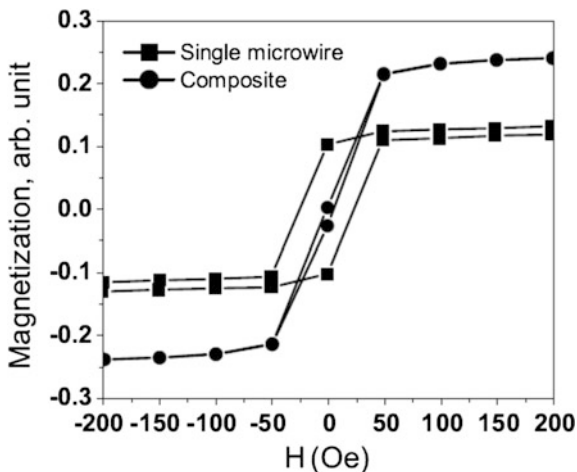
[11]. Such changes of magnetostatic and magnetoelastic characteristics are due to the long-range dipolar interactions [7, 12] between neighbouring wires, as well as the interfacial stress between microwires and the matrix. The dipolar interactions have a strong impact on the magnetic properties in a similar way to classical spins interacting throughout the long-range interactions, resulting in the changes in the hysteresis loop. Equally, interfacial stress of the order of hundreds of MPa [13, 14], resulting from the different coefficients of thermal expansion between the microwire and polymer matrix, will have a significant effect on the magnetoelastic features of the wires according to $K_{me} = 3/2\lambda(\sigma_i + \sigma_{app})$, where K_{me} is the magnetoelastic energy component, λ is the magnetostriction constant, and σ_i and σ_{app} are the internal stress and applied stress on the wire, respectively [15, 16]. In the case of Fe-based wire of a length greater than the critical length, due to the dipolar interactions, the coercivity and anisotropy field should increase with the number of wires. On the other hand, the coercivity is decreased with increasing stress, and anisotropy presents an opposite trend [13, 15, 17]. The combination of these two mechanisms results in the observed contrast between the microwire composites and monolithic wire. The presented magnetic properties indicate that the microwire composites are promising for magnetic sensing applications [18].

Due to the involvement of the polymer, magnetic filler, and multi-interfaces, temperature plays an important role in regulating the magnetic behaviour of composites. The glass transition temperature (tg) of the composite samples is evaluated to gain a better understanding of their magnetic properties (see Fig. 10.2). Phan et al. found that, by annealing in the vicinity of the glass transition temperature, there exists a critical temperature of 177 °C. Before the temperature reaches this, the coercivity decreases, while afterwards the opposite trend is shown. This is contrary to the conventional case that the coercivity should decrease with the stress relaxation due to the thermal annealing below the crystallisation temperature [19]. Clearly, such a complex annealing temperature dependence of coercivity involves

Fig. 10.2 Magnetic
hysteresis loops of the
as-prepared composite
annealed at Ta = 375, 405,
and 435 K. The glass
transition temperature is
449.5 K. Reproduced with
permission from [10],
copyright 2007 AIAA
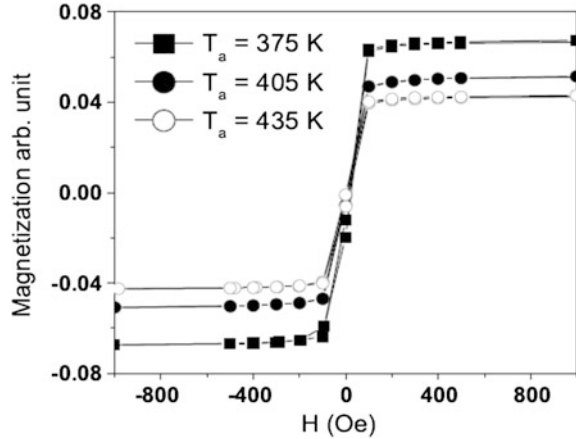
multiple mechanisms at different interfaces, viz. the structural relaxation in the wire
and the stress relief in the polymer–wire interface. The competitive and interde-
pendent relationship between these two mechanisms varies sensitively with the
temperature. At low temperatures relative to the glass transition temperature, the
second mechanism prevails and can result in a rearrangement of microwires, i.e.
regulation of the composite mesostructure. Thus, the coercivity could be increased
due to the enhanced interaction between the wires [20]. Subsequently, a decrease of
coercivity should result from the stress relief contributed by both glass transition
and wire structural relaxation. The gradual decrease of remanent magnetisation can
be accounted for by the reduction in the volume of the axially magnetised area as an
effect of stress relief due to the positive magnetostriction constant [15, 17].

10.2   Giant Magnetoimpedance Effect

As with wires, their composite also presents a significant GMI effect. It has been
shown by Phan et al. [10] that, at a given frequency of 10 MHz, the GMI ratio and
its field sensitivity reached the highest values of 450 and 45 %/Oe for those
composites containing four wires, while the composite containing only one wire
gave 14 and 1 %/Oe, respectively (see Fig. 10.3). The wire addition effect on the
GMI is believed to be attributed to the reduction in resistivity as one of the causes.
Another cause is the combination of the high circumferential permeability of the
microwire, and a multiwire parallel configuration is likely to cause a magnetic flux
closure and hence resulted in an extremely high effective permeability [20, 21]. It is
worth noting both GMI and anisotropy field are enhanced, which is highly desirable
for realising high-performance sensing entailing large sensitivity and broad working
range. In addition, compared to single wire, the existence of polymer matrix could
accommodate a versatile and judiciously designed multiwire system, which

Fig. 10.3 Frequency dependence of GMI profiles with varying wire number $n = 1, 2, 3, 4$ mm. Reproduced with permission from [24], copyright 2007 Elsevier
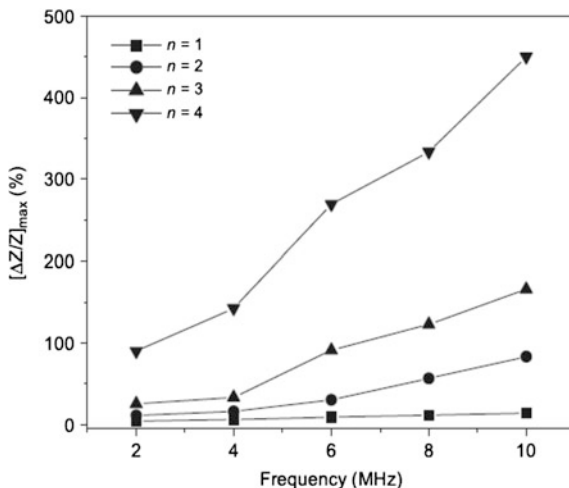
provides more possibility to extend its applications. However, the GMI presented in Ref. [10] is very weak, with the suitable optimisation of single wires via advanced annealing techniques such as stress–Joule annealing [22] and recently reported multiangle annealing techniques [23], and the GMI of wire composite could be further improved.

Qin et al. [25] also demonstrated the pronounced improvement of the maximum MI ratio with the increasing number of wire inclusions, attributed to the effective response of all the wires. The microwire composite is shown to yield a larger GMI at higher frequencies but with a minor increase of energy loss, which is desirable for sensing applications. The multiwires in the parallel manner constitute an increase of the total cross-sectional area of the wires, resulting in a stronger skin effect when considering the ratio of radius and penetration depth. Consequently, the GMI effect is improved. In addition, if the wire is simply dealt with as a single-domain sub-stance, the interactions between wires in the multiwire composites induce a mag-netic closure to make the whole structure more stable, although the total internal energy is increased [12]. These results differ significantly from those reported by Garcia [26], who demonstrated a multiwire system exhibiting a reduced GMI effect with the number of wires, which is explained by the authors as an effect of shielding between wires. This difference should be ascribed to the functions of the matrix and the curing process for our composite media. The wire sample underwent annealing in the curing stage, and the domain structure was significantly modified. It is suggested that the confinement of the matrix also helps maintain the modified configuration, giving rise to the peculiarity of the GMI behaviour. Of note is that the involvement of a polymer matrix opens up new routes to modulate the GMI performance, although limited study has been hitherto reported. A particularly important aspect is interface. The homogeneities of the interface would be critical to the GMI characteristics, so it is necessary to study the detailed interfacial

conditions. Surface treatment using chemical agents such as silane or nanotubes [27] could also be considered to enhance both the interfacial bonding and GMI properties. Another aspect of practical interest [28, 29] is to develop superior bonding technology to accommodate multiple wires so that a highly stable GMI signal output can be ensured.

It is well established that the GMI effect of microwires associated with the magnetic properties is strongly influenced by the length of the wires [3, 30–33]. The argument holds true for the microwire composite system. It has been revealed that the GMI ratio increased from 15.5 to 268 % as the microwire length decreased from 4 to 1 mm [10]. This is attributed to the decrease of the electric resistivity in the multiwire system compared to the single wire, in spite of the increase of the demagnetising effect [3] for single wire. Based on the outstanding magnetic properties of microwire composites, they show a promising application perspective. Indeed, the polymer matrix provides a "platform" to assemble the microwires and exhibit the properties that are significantly different from the single wire, which is the motivation for developing these composites [34].

10.3   Giant Stress Impedance Effect

As mentioned above, stresses can play an important role in investigating the GMI materials, and these can be treated in two respects. One concerns the stress influence on the GMI behaviour, and a number of works have been published on this topic for various materials including ribbons [35–37] and microwires [38–40]. Second is the so-called giant stress impedance (GSI) effect, which refers to a stress-induced variation of impedance in magnetic materials. This effect in the intermediate frequencies has been evaluated on amorphous wires and ribbons. Shen [41] reported that the GSI effect of a CoSiB microwire reached about −35 % for stress $\sigma = 140$ MPa, which is 5–6 times more sensitive than a conventional semiconductor stress sensor. One kind of Fe-based ribbon was also found to possess an SI ratio of 20 % for $\sigma = 84.8$ MPa with the stress perpendicular to the geomagnetic field [42]. In this regard, the wire-based composite is expected to be a good candidate for studying the GSI effect over a wider stress range, since it can be treated as a multilayer medium consisting of a metallic core, a glass coat, and a composite matrix. Such a hierarchical structure would enable a sensitive response to the applied stress for the composite media, where the coupling of internal and external stresses is likely to be able to manipulate the GMI and GSI behaviour. Both aspects of the GSI effect of microwire composites were investigated by Qin et al. [13].

Figure 10.4 illustrates the magnetic field dependence of the GMI ratio taken at $f = 1$ MHz under various applied tensile stresses for the single-wire composite of four layers obtained by the method described in Sect. 9.2.2. Here, the tensile stress was applied along the microwire axis. It can be seen from the figure that the maximum GMI ratio decreased as the applied stress was increased. While the GMI ratio decreased gradually with the applied magnetic field (H_{dc}) for the unstressed

Fig. 10.4 GMI profiles of composites containing single wire as a function of applied stress. Reproduced with permission from [13], copyright 2011 Elsevier
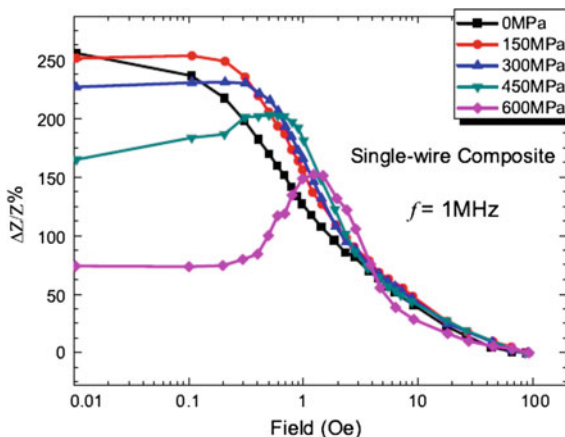
composite, the case is different for the stressed composites. With increasing H_{dc}, the GMI ratio first increased, then reached a maximum, and finally decreased for the stressed composites. The magnetic field at which the GMI ratio reached its maximum can be considered as the circular anisotropy field (H_k) induced by the applied tensile stress.

Figure 10.5a illustrates the tensile stress dependence of the maximum GMI ratio and the anisotropy field. Clearly, the GMI ratio decreased slightly from 255 % for $\sigma = 0$ to 253 % for $\sigma = 150$ MPa and drastically reduced to 151 % for $\sigma = 600$ MPa by more than 100 %. An opposite trend was observed for the σ dependence of H_k.


Fig. 10.5 a Tensile stress dependences of anisotropy field (H_k) determined from GMI profiles and maximum GMI ratio. **b** Longitudinal coercivity versus applied tensile stress. Reproduced with permission from [13], copyright 2011 Elsevier
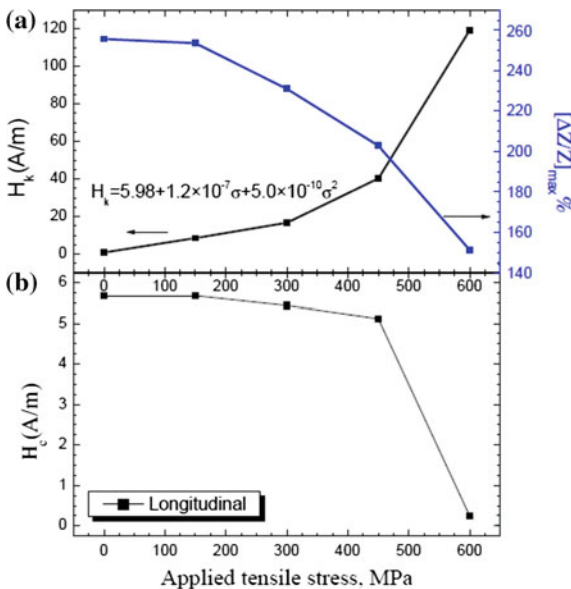
A subtle increase of H_k by 8A/m for $\sigma = 150$ MPa was followed by a further increase of 112 A/m for $\sigma = 600$ MPa. The σ dependence of longitudinal coercivity (H_c) was also measured, and the result is shown in Fig. 10.5b. The drop of H_c was observed at $\sigma = 600$ MPa. For the case of the unstressed composite, the gradual decrease of the GMI ratio with H_{dc} is likely to be caused by decreasing circular permeability due to the rotation of magnetic moments. However, an opposite effect observed for the stressed composites arises from the fact that the application of tensile stress to the microwire with a negative magnetostriction strengthened the circular magnetoelastic anisotropy field, giving rise to the occurrence of a maximum in GMI that shifted towards higher H_{dc} as σ was increased. The occurrence of such a maximum in GMI for the stressed composites can be attributed to the competition in the rotational magnetisation processes between H_{dc} and H_k. The decrease of the GMI ratio with σ at $H_{dc} = 0$ is attributed to a reduction in the circular permeability due to the domain wall displacement.

Furthermore, it should be noted that, since the microwires were embedded in a polymer matrix, any heat treatment or variation coming from the polymer matrix is expected to have a significant influence on the GMI properties of the microwire and hence the composite. To gain insight into this, the influences of annealing treatment and the number of layers on the GMI properties are studied. The results are shown in Fig. 10.6. For the case of the as-prepared samples, the four-layer composite exhibited a higher maximum GMI ratio (255 %) when compared with the eight-layer composite (216 %). Meanwhile, the annealed composite samples (treated at 100 °C for 3 h) exhibited higher maximum GMI ratios (282 and 248 % for the four-layer and eight-layer composites, respectively) than the as-prepared ones. These findings are explained as follows. In this kind of composite, a higher stress will be induced as the number of composite layers increases. In the present study, the eight-layer composite may impose more stress in the through-thickness direction than the four-layer composite. As a result, the GMI ratio decreased and H_k increased for the as-prepared composite of eight layers when compared with the as-prepared composite of four

Fig. 10.6 GMI profiles for the wire composites of four prepreg layers and eight prepreg layers in the as-prepared and annealed states taken at $f = 1$ MHz. Reproduced with permission from [13], copyright 2011 Elsevier
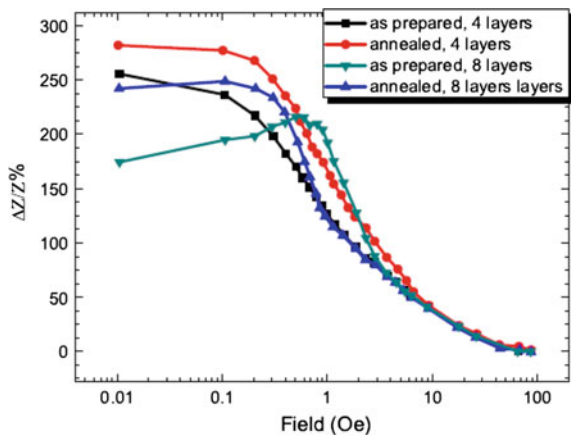
layers. On the other hand, the annealing treatment is believed to have relieved the stress between the microwire and matrix produced during the curing process. This explains consistently the larger GMI ratio and smaller H_k obtained for the annealed composite samples relative to the as-prepared ones.

It is also interesting to see that the GMI behaviour observed for the as-prepared eight-layer composite is similar to that of the four-layer composite subject to a tensile stress of 450 MPa. This clearly suggests that the applied tensile stress and residual stress imposed by the composite matrix on the microwire could affect its GMI behaviour in a similar fashion. To understand this quantitatively, the contribution of the applied stress and the matrix-induced residual stress to the anisotropy field was calculated, respectively.

In a cylindrical coordinate system (z, r, ϕ), there exist three components for the residual stress in z (along the wire axis), r (radial direction), and ϕ (azimuthal direction): zz, rr, and $\phi\phi$, respectively. The magnetoelastic energy density is given by Antonov et al. [43]:

$$U_{\text{me}} = -\frac{3}{2}\lambda_{\text{s}}(\sigma_{zz}\alpha_z^2 + \sigma_{rr}\alpha_r^2 + \sigma_{\phi\phi}\alpha_\phi^2), \qquad (10.2)$$

where λ_{s} is the saturation magnetostriction constant. α_i denotes the component of the unit magnetisation vector. The residual stresses are assumed to be a function of $x(r/a)$ only, a being the wire radius.

The anisotropy field can then be deduced by the following equation [43]:

$$H_k = \frac{3|\lambda_{\text{s}}|}{M_{\text{s}}}\left(\sigma_{zz} - \sigma_{\phi\phi} + \frac{1}{(1-k)p^2+k}\overline{\sigma_{zz}}\right), \qquad (10.3)$$

where all symbols have the same meaning as in Eq. (10.2).

Taking into account the residual stress imposed by the composite matrix, which is primarily along the negative radial direction (σ_{rr}), Eq. (10.3) can be modified to the following:

$$H_k = \frac{3|\lambda_{\text{s}}|}{M_{\text{s}}}\left(\sigma_{zz} - \sigma_{\phi\phi} + \overline{\sigma_{rr}} + \overline{\overline{\sigma_{zz}}}\right); \qquad (10.4a)$$

$$\overline{\overline{\sigma_{zz}}} = \frac{1}{(1-k)p^2+k}\overline{\sigma_{zz}}. \qquad (10.4b)$$

For the four-layer composite, when $\overline{\sigma_{zz}} = 450$ MPa, given $k = 0.5$ and $p = 0.67$, one obtains the effective contribution to H_k, $\overline{\overline{\sigma_{zz}}} = 619$ MPa. For the eight-layer composite, according to the difference of its anisotropy field relative to that of the unstressed four-layer composite ($\Delta H_k = 0.5$ Oe), the concerned stress $\overline{\sigma_{rr}}$ is given by the following:

Fig. 10.7 GSI profiles for amorphous wire, four-layer wire composite, and eight-layer wire composite in the as-prepared states taken at $f = 1$ MHz. Reproduced with permission from [13], copyright 2011 Elsevier
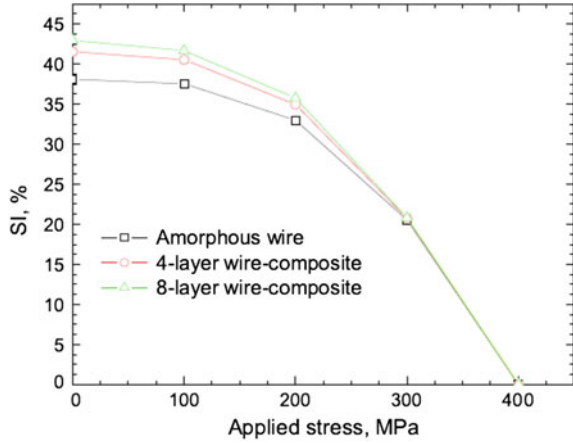
$$\overline{\sigma_{rr}} = \frac{\Delta H_k M_s}{3|\lambda_s|}. \tag{10.5}$$

Given the typical numerical values: $M_s = 400\ G$, $\lambda_s = -10^{-7}$, $\overline{\sigma_{rr}} = 667$ MPa is received. The similar numerical values of $\overline{\sigma_{rr}}$ and $\overline{\overline{\sigma_{zz}}}$ explain the roles of applied stress and residual stress in influencing the magnetoelastic properties and GMI properties. This result affords significant technical applications in the composite industry in terms of probing the residual stress and tailoring the related manufacturing conditions.

The GSI effect in the microwire and the microwire-based composites with four and eight layers was investigated. The results are shown in Fig. 10.7. It can be readily seen that the stress impedance ratio $[\Delta Z/Z]_{max}$ decreased monotonously with stress for all the samples. Interestingly, while the maximum stress impedance ratio ($[\Delta Z/Z]_{max}$) is 38.1 % for the single microwire, it is reinforced for the composite samples (41.5 and 43.0 % for the four-layer and eight-layer composites, respectively). These results indicate that the prepared composites are very appealing candidates for the stress-sensing applications. In the composite, in addition to the residual stress frozen in between the glass and metallic core, there exists residual stress at the interface between the microwire and polymer matrix. The enhancement of the GSI effect in the composites clearly points to the important coupling between the internal and external stresses that coexist in these materials.

10.4   Mechanical Properties

Since the fabricated composite is intended for structural applications, its mechanical properties are one of the major concerns. Also, the influence of microwires on the mechanical integrity of the composite is a key issue for the success of such
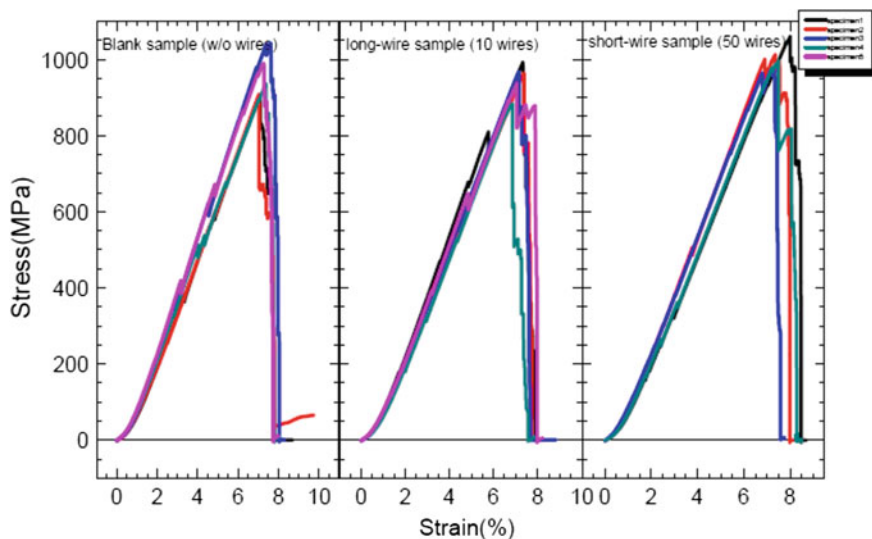
Fig. 10.8 Stress–strain curves of blank composites (free of wires), composites containing 10 wires and 50 wires measured by a 30 kN load cell. Reproduced with permission from [25], copyright 2010 Elsevier

sensor-embedded technology. Therefore, it is necessary to discuss the mechanical properties of the composite matrix influenced by the embedded wires [25, 44–46].

Qin et al. [25, 46] found that, in a dilute composite with glass fibre-reinforced epoxy as a matrix, the fibre shows little effect, as shown in Fig. 10.8, which displays the stress–strain curves obtained for blank composite samples and 10-wire and 50-wire samples under a maximum force of 30 kN [25]. The tensile strengths are summarised in Table 10.1. It is observed that all the mechanical parameters are very close to each other for the different types of samples. In terms of the tensile strength, the coefficients of variation (CV) for each type of sample are 6.3, 5.6, and 3.8. Upon performing cross-comparison of their average properties, the CV is 3.7. The negligible wire effect can be understood from the basic law of mixture that postulates a considerable volume fraction of fillers needed to realise reinforcement.

Qin et al. [47] also studied the impact resistance of this kind of microwire composite. With reference to the obtained time dependences of the impact force for all tested samples (Fig. 10.10), one can see that the additional wires yield negligible changes in the impact resistance of the composites parametrised by the impact

Table 10.1 Mean values and coefficients of variation (CV*) of tensile strength for each set of samples

	Blank sample	10-wire sample	50-wire sample
Young's modulus (GPa)	14.22 (3.1*)	14.48 (1.1)	14.97 (3.0)
Tensile strength (MPa)	951.48 (6.3)	935.18(5.6)	1003.80(3.8)

The asterisk (*) is used to indicate that the number in the parenthesis is coefficient of variation, i.e. CV

energy, in that the major energy dissipation mechanism is delamination rather than fibre failure, as shown in a typical damage pattern at the surface (inset of Fig. 10.10; the bright region indicates the delamination). This suggests that the embedded wires do not degrade the interfacial bonding. This is of particular importance for aeronautical structures that are subject to low-velocity impact caused by, e.g., dropped tooling or runway debris, throughout their service life [48]. Another notable feature concerns the first load peak, which exhibits a significant increase for the sample containing three layers of wires as compared to other samples. This clearly indicates that the fibre failure occurred near the surface as the initial impact damage [49]. The metallic wires with the strong tensile strength of 3–4 kMPa effectively improve the fracture load. It can be expected that, for high-velocity impact, the addition of wires can also improve the toughness of the composites. In considering the wide application of glass fibre composites in wind turbines, the addition of microwires can simultaneously improve the impact resistance performance and electromagnetic interference shielding (this will be discussed in Chap. 12) of the composites, rendering such microwire composites particularly useful for improving on the current green energy technology.

Back in the 1980s, Goto et al. [44, 45] had done excellent work in connection with the mechanical performance of metallic filament-reinforced composites. Goto et al. [44] studied the reinforcing effect of metallic wires with and without glass coats on the epoxy matrix and reported that the mechanical properties of epoxy are strongly enhanced in wires without a glass coating, with the tensile strength reaching 600 MPa at 30 vol.% wire volume. Meanwhile, the glass-coated wires do not show such a good reinforcing effect due to the poor bonding between the metallic core and glass coating. These effects are readily demonstrated in the fracture morphology images (Fig. 10.9). Apparently, the quality of the interfaces plays a critical role in determining the ultimate mechanical performance of the wire composites. These fine wires, after removing the glass coating, are also found to be capable of improving the thermal properties of the composite by increasing the
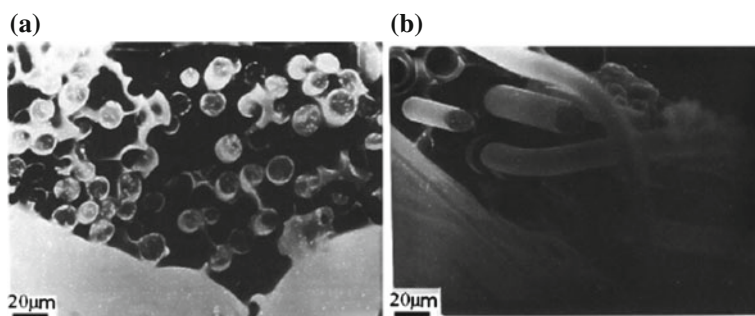

Fig. 10.9 Fracture morphology of microwire (glass coat removed)/epoxy composite (**a**) and glass-coated microwire/epoxy composite (**b**). Reproduced with permission from [44], copyright 1987 Springer
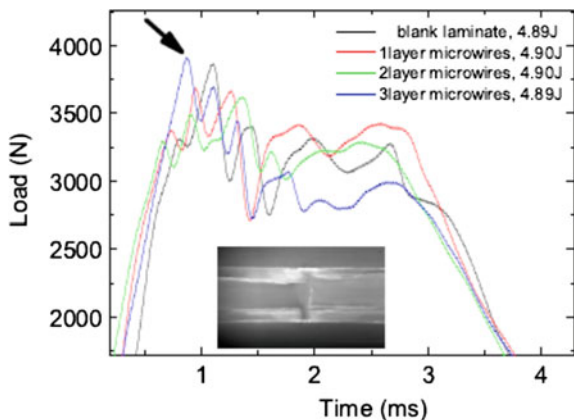
Fig. 10.10 Time dependence of impact force for blank sample and heavily wire-loaded composites containing one layer of microwires (embedded depth $h = 1$ mm), two layers ($h_1 = 0.75$ mm $h_2 = 1.25$ mm), and three layers ($h_1 = 0.5$ mm, $h_2 = 1$ mm, $h_3 = 1.5$ mm). Each layer contains 200 microwires. The inset shows in-plane view of the damaged spot in the 950 E-glass laminates after the impact test

glass transition temperature, as the wires can hinder the molecular motion (Fig. 10.10).

Although the microwires can reinforce the polymer materials with adequate concentration and proper orientation, a trade-off is often inevitable if one tends to integrate the structural function and other functionalities which do not necessarily favour a large concentration or unidirectional fillers. For the designers of such multifunctional composites, it is necessary to maximise the most desirable function for the targeted application, while keeping the cost of other functionalities as low as possible.

References

1. Sihvola A, Lindell I (1992) Effective permeability of mixtures Prog Electromagn Res 1–36
2. Laroze D, Escrig J, Landeros P, Altbir D, Vázquez M, Vargas P (2007) A detailed analysis of dipolar interactions in arrays of bi-stable magnetic nanowires. Nanotechnology 18:415708
3. Di Y, Jiang J, Bie S, Yuan L, Davies HA, He H (2008) Collective length effect on the magnetostatic properties of arrays of glass-coated amorphous alloy microwires. J Magn Magn Mater 320:534–539
4. Vázquez M (2001) Soft magnetic wires. Phys B 299:302–313
5. Sampaio LC, Sinnecker EHCP, Cernicchiaro GRC, Knobel M, Vázquez M, Velázquez J (2000) Magnetic microwires as macrospins in a long-range dipole-dipole interaction. Phys Rev B 61:8976–8983
6. Velazquez J, Vazquez M, Zhukov A (1996) Magnetoelastic anisotropy distribution in glass-coated microwires. J Mater Res 11:2499–2505

7. Velazquez J, Garcia C, Vazquez M, Hernando A (1999) Interacting amorphous ferromagnetic wires: a complex system. J Appl Phys 85:2768–2774
8. Acher O, Dubourg S (2008) Generalization of snoek's law to ferromagnetic films and composites. Phys Rev B 77:104440
9. Acher O, Adenot AL (2000) Bounds on the dynamic properties of magnetic materials. Phys Rev B 62:11324–11327
10. Phan M, Peng H, Wisnom M, Mellor P (2007) Optimizing the nano-structure of magnetic micro-wires for multifunctional macro-composites. AIAA-2007-2032 48th Qin, Phan and Peng, submitted to Springer AIAA/ASME/ASCE/AHS/ASC Structures, Structural Dynamics, and Materials Conference, Honolulu, Hawaii
11. Di Y, Jiang J, Du G, Tian B, Bie S, He H (2007) Magnetic and microwave properties of glass-coated amorphous ferromagnetic microwires. Trans Nonferrous Met Soc China 17:1352–1357
12. Velázquez J (1996) Dynamic magnetostatic interaction between amorphous ferromagnetic wires. Phys Rev B 54:9903–9911
13. Qin F, Peng H, Popov V, Phan M (2011) Giant magneto-impedance and stress-impedance effects of microwire composites for sensing applications. Solid State Commun 151:293–296
14. Qin FX, Peng HX, Popov VV, Panina LV, Ipatov M, Zhukova V, Zhukov A, Gonzalez J (2011) Stress tunable properties of ferromagnetic microwires and their multifunctional composites. J Appl Phys 108:07A310
15. Zhukova V, Zhukov A, Blanco JM, Gonzalez J, Gomez-Polo C, Vazquez M (2003) Effect of stress applied on the magnetization profile of Fe–Si–B amorphous wire. J Appl Phys 93:7208–7210
16. Zhukov A, Ipatov M, Gonzalez J, Blanco JM, Zhukova V (2009) Recent advances in studies of magnetically soft amorphous microwires. J Magn Magn Mater 321:822–825
17. Zhukova V, Larin VS, Zhukov A (2003) Stress induced magnetic anisotropy and giant magnetoimpedance in Fe-rich glass-coated magnetic microwires. J Appl Phys 94:1115–1118
18. Vazquez M, Hernando A (1996) A soft magnetic wire for sensor applications. J Phys D: Appl Phys 29:939–949
19. Zhukova V, Cobeno AF, Zhukov A, Blanco JM, Larin V, Gonzalez J (1999) Coercivity of glass-coated Fe73.4-xCu1Nb3.1Si13.4 + xB9.1 (0 <=x <=1.6) microwires. Nanostruct Mater 11:1319–1327
20. Chizhik A, Zhukov A, Blanco JM, Szymczak R, Gonzalez J (2002) Interaction between Fe-rich ferromagnetic glass-coated microwires. J Magn Magn Mater 249:99–103 (Qin, Phan and Peng, submitted to Springer)
21. Amalou F, Gijs MAM (2002) Giant magnetoimpedance in trilayer structures of patterned magnetic amorphous ribbons. Appl Phys Lett 81:1654–1656
22. Kraus L, Chiriac H, Ovari TA (2000) Magnetic properties of stress-joule-heated amorphous fecrbsimicrowire. J Magn Magn Mater 215–216:343–345
23. Liu J, Cao F, Chen D, Xue X, Sun J (2012) Multiangle combined magnetic-field annealing of Cobased amorphous microwires for sensor applications. Phys Status Solidi A 209:984–989
24. Phan M, Peng H, Yu S, Wisnom M (2007) Large enhancement of GMI effect in polymer composites containing Co-based ferromagnetic microwires. J Magn Magn Mater 316:e253–e256
25. Qin F, Peng HX, Tang J, Qin LC (2010) Ferromagnetic microwires enabled polymer composites for sensing applications. Compos A Appl Sci Manuf 41:1823–1828
26. Garcia C, Zhukova V, Zhukov A, Usov N, IpatovM, Gonzalez J, Blanco J (2007) Effect of interaction on giant magnetoimpedance effect in a system of few thin wires. Sens Lett 5:10–12
27. Chaturvedi A, Stojak K, Laurita N, Mukherjee P, Srikanth H, Phan MH (2012) Enhanced magnetoimpedance effect in co-based amorphous ribbons coated with carbon nanotubes. J Appl Phys 111:07E507
28. Liu J, Wang X, Qin F, Xing D, Cao F, Peng H, Xiang X, Sun J (2011) Gmi output stability of glasscoated co-based microwires for sensor application. PIERS Online 7:661–665

29. Liu JS, Sun JF, Xing DW, Xue X, Zhang SL, Wang H, Wang XD (2011) Experimental study on the effect of wire bonding by cu electroplating on gmi stability of co-based amorphous wires. Physica status solidi (a) 208:530–534
30. Qin F, Peng H, Phan M (2010) Wire-length effect on gmi in co70.3fe3.7b10si13cr3 amorphous glasscoated microwires. Mater Sci Eng B 167:129 – 132
31. Severino AM, Gomez-Polo C, Marin P, Vazquez M (1992) Influence of the sample length on the switching process of magnetostrictive amorphous wire. J Magn Magn Mater 103:117–125
32. Vazquez M, Li YF, Chen DX (2002) Influence of the sample length and profile of the magnetoimpedance effect in fecrsibcunb ultrasoft magnetic wires. J Appl Phys 91:6539–6544
33. Zhukova V, Usov NA, Zhukov A, Gonzalez J (2002) Length effect in a co-rich amorphous wire. Phys Rev B 65:134407
34. Ajayan PM, Tour JM (2007) Materials science: nanotube composites. Nature 447:1066–1068
35. Coisson M, Tiberto P, Vinai F, Kane S (2003) Influence of stress-annealing on magneto-transport properties in co-based amorphous ribbons. Sens Actuators A 106:199–202
36. Ohnuma M, Hono K, Yanai T, Nakano M, Fukunaga H, Yoshizawa Y (2005) Origin of the magnetic anisotropy induced by stress annealing in Fe-based nanocrystalline alloy. Appl Phys Lett 86:152513
37. Fels A, Friedrich K, Hornbogen E (1984) Reinforcement of a brittle epoxy resin by metallic glass ribbons. J Mater Sci Lett 3:569–574
38. Mandal K, Mandal SP, Vázquez M, Puerta S, Hernando A (2002) Giant magnetoimpedance effect in a positive magnetostrictive glass-coated amorphous microwire. Phys Rev B 65:064402
39. Blanco JM, Barbon PG, Gonzalez J, Gomez-Polo C, Vazquez M (1992) Stress induced magnetic anisotropy in non-magnetostrictive amorphous wires. J Magn Magn Mater 104–107:137–138
40. Cobeno AF, Zhukov A, Blanco JM, Larin V, Gonzalez J (2001) Magnetoelastic sensor based on GMI of amorphous microwire. Sens Actuators A 91:95–98
41. Shen L, Uchiyama T, Mohri K, Kita E, Bushida K (1997) Sensitive stress-impedance micro sensor using amorphous magneostrictive wire. IEEE Trans Magn 33:3355–3357
42. Hu J, Qin H, Chen J, Zhang Y (2003) Giant stress-impedance effect in Fe73.5CuNb3-xVxSi13.5B9 amorphous ribbons. J Magn Magn Mater 266:290–295
43. Antonov AS, Borisov VT, Borisov OV, Prokoshin AF, Usov NA (2000) Residual quenching stresses in glass-coated amorphous ferromagnetic microwires. J Phys D Appl Phys 33:1161
44. Goto T, Nishio K (1987) Mechanical properties of high strength and high toughness metallic filament composites with epoxy and poly(ether ether ketone) matrices. J Mater Sci 22:2357–2362
45. Goto T, Tsubouchi H (1988) High temperature mechanical properties of high toughness metallic filament composites with polyimide and epoxy matrices. J Mater Sci 23:3630–3635
46. Qin F, Peng H (2010) Macro-composites containing ferromagnetic microwires for structural health monitoring. Nano Commun Netw 1:126–130
47. Qin F, Peng H, ZChen, Wang H, Zhang J, Hilton G (2013) Optimization of microwire/glass-fiber reinforced polymer composites for wind turbine application. Appl Phys A Mater Sci Process. 10.1007/s00339-013-7820-2
48. Guinard S, Allix O, Guedra-Degeorges D, Vinet A (2002) A 3d damage analysis of low-velocity impacts on laminated composites. Compos Sci Technol 62:585–589
49. Breen C, Guild F, Pavier M (2005) Impact of thick cfrp laminates: the effect of impact velocity. Compos A Appl Sci Manuf 36:205–211